Current Biology *16*, 1161–1170, June 20, 2006 DOI 10.1016/j.cub.2006.04.040

Article

Dynamics of the Formin For3p in Actin Cable Assembly

Sophie G. Martin[1] **and Fred Chang**[1,*]
[1] Department of Microbiology
College of Physicians and Surgeons
Columbia University
701 West 168th Street
New York, New York 10032

Summary

Background: Formins are a conserved family of actin nucleators responsible for the assembly of diverse actin structures such as cytokinetic rings and filopodia. In the fission yeast *Schizosaccharomyces pombe*, the formin for3p is necessary for the formation of actin cables, which are bundles of short parallel actin filaments that regulate cell polarity. These filaments are largely organized with their barbed ends facing the cell tip, where for3p is thought to function in their assembly.
Results: Here, using a functional for3p-3GFP fusion expressed at endogenous levels, we find that for3p localizes to small dots that appear transiently at cell tips and then move away on actin cables at a rate of 0.3 μm/s. These movements were dependent on the continuous assembly of actin in cables, on the ability of for3p to bind actin within its FH2 domain, and on profilin and bud6p, two formin binding proteins that promote formin activity. Bud6p transiently colocalizes with for3p at the cell tip and stays behind at the cell tip when for3p detaches.
Conclusions: These findings suggest a new model for actin cable assembly: a for3p particle is activated and promotes the assembly of a short actin filament at the cell tip for only seconds. For3p and the actin filament may then be released from the cell tip and carried passively into the cell interior by retrograde flow of actin filaments in the cable. These studies reveal a complex and dynamic cycle of formin regulation and actin cable assembly in vivo.

Introduction

Distinct sets of actin-organizing proteins function to shape the diverse actin structures in the cell. Formins are key actin filament nucleators that participate in the assembly of many actin structures [1]. Generally, these large multidomain proteins have the ability to nucleate actin filaments and bind stably to the growing barbed end of the filament, through their formin-homology 2 (FH2) domain, to promote actin elongation and prevent binding of capping protein [2–6]. The adjacent FH1 domain binds profilin, an abundant actin monomer-associated protein, which promotes nucleotide exchange on actin, and profilin increases the rate of formin-mediated barbed end elongation [7–9]. In vitro, FH1-FH2 fragments of several formins have been shown to remain tightly associated with the barbed end of elongating filaments for several minutes, even as the filament grows over 10 μm [7, 9–11]. In vivo, fragments of the formin mDia1 form particles that display actin-dependent movements [11].

One important question is how is the activity of formins spatially controlled in vivo. Regulation of formins may be a critical way to control actin assembly in the cell. Many formins bind to small GTPases such as Rho and Cdc42 proteins, which regulate autoinhibitory intramolecular interactions in the formin through its DID and DAD domains [12–14]. However, it is likely that additional modes of regulation are also present. For instance, the yeast formin Bni1p binds Bud6p, a protein that, similar to profilin, promotes nucleotide exchange on actin monomers and enhances formin activity in vitro [6].

The fission yeast *Schizosaccharomyces pombe* possesses three formins, each responsible for the formation of a distinct actin structure. The formin for3p is necessary for the formation of actin cables and for polarized cell growth [15, 16]. A recent electron microscopy study showed that these cables are composed of bundles of short linear actin filaments [17]. Myosin S1 decoration revealed that within an actin cable most (but not all) of the individual filaments are oriented in a parallel manner with their barbed (fast growing) ends facing the growing cell tips during interphase and facing the site of cell division during cytokinesis [17]. Actin cables are not essential for cell viability in fission yeast but contribute to polarized cell growth and serve as tracks for the delivery of myosin V-driven vesicles to the sites of cell growth [16, 18] (S. Salas-Pino and F.C., unpublished data) and for the Arp2/3-dependent movement of actin patches (endocytic organelles) toward the cell interior [19].

The spatial and temporal regulation of for3p is likely to be critical for proper organization and function of actin cables in polarized growth. For instance, the targeting of for3p by the microtubule plus-end factors tea4p and tea1p is sufficient for the establishment of cell polarity during new end take off (NETO) [20, 21]. For3p has been shown to interact with both rho3p and cdc42p, but the significance of these interactions is not yet well understood [15, 20, 22]. For3p also interacts with bud6p (the homolog of budding yeast Bud6p), which is necessary for efficient actin cable formation in vivo [21]. Similar to the budding yeast formins, previous studies with for3p-YFP showed a crescent-shaped localization pattern of for3p at the cortex of growing cell tips and to the cytokinetic ring during mitosis [16, 23, 24]. This localization pattern was consistent with the apparent assembly of actin cables from the cell tips and with the orientation of barbed ends of actin filaments facing the cell tips. However, the dim fluorescence of for3p-YFP and the long exposure times needed to visualize the protein precluded us from studying more rapid dynamics.

Here, we investigated the dynamics of for3p by using a full-length for3p tagged with three tandem copies of

*Correspondence: fc99@columbia.edu

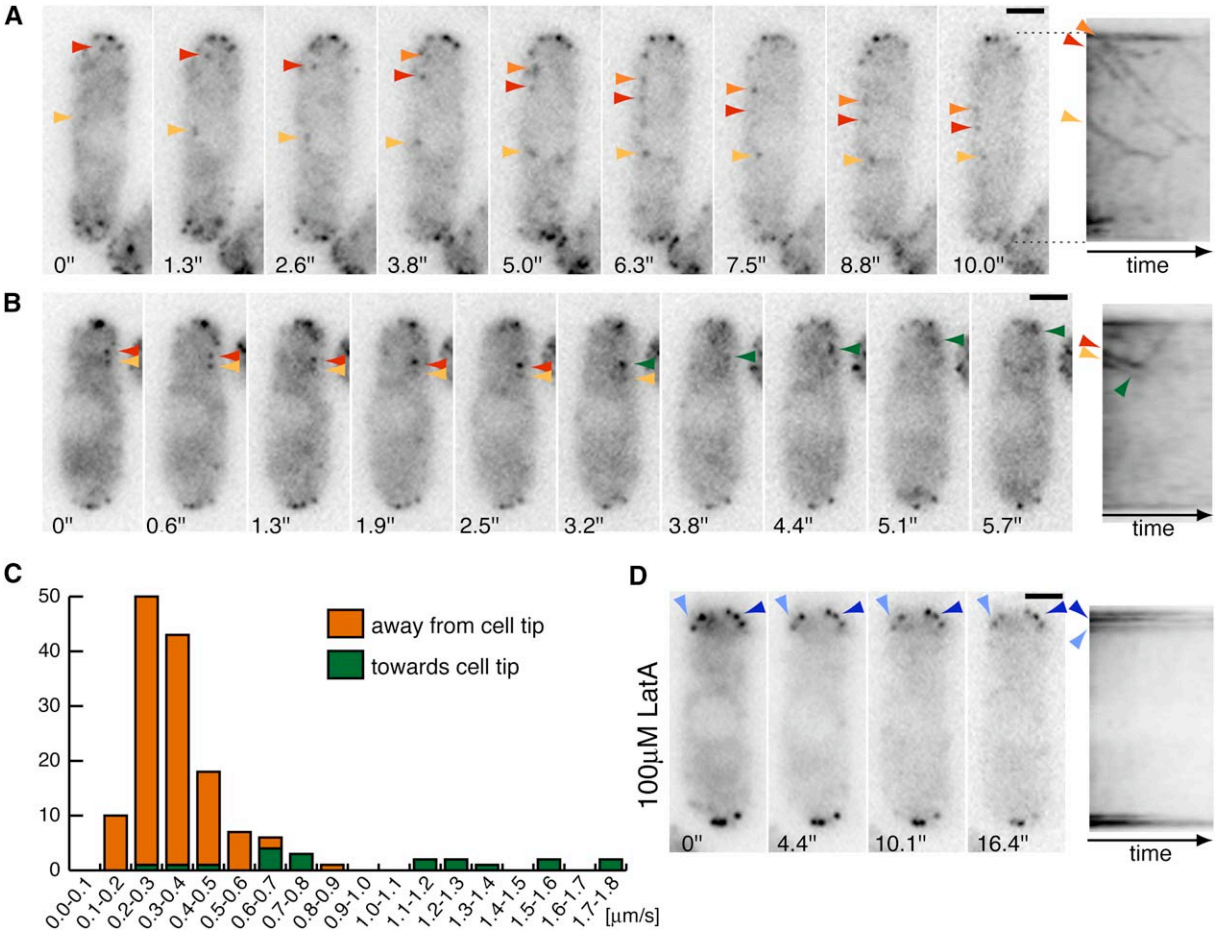

Figure 1. Formin For3p Movements

(A and B) For3p-3GFP expressing cells were imaged in a single focal plane on a wide-field microscope. Time-lapse images and corresponding kymographs are shown. Arrowheads indicate individual for3p dots and their corresponding trace in the kymograph. Yellow, orange, and red colored bars and arrows refer to for3p dots moving away from the cell tip. Green refers to for3p dots moving toward the cell tip. Time is indicated in seconds. Note that the time scale in each kymograph is different in each panel.

(C) Histogram distribution of for3p-3GFP dot rates.

(D) Time-lapse images of for3p-3GFP and kymograph treated with 100 μM LatA for 5 min, showing that for3p movements depend on F-actin. Note that all for3p particles are static at cell tips (two are highlighted by blue arrowheads). Scale bars represent 2 μm.

GFP. The substantially brighter fluorescence and more rapid image acquisition in time-lapse fluorescence microscopy allowed us to visualize for3p behaviors that were not detectable with the previous fusion. The movements of for3p particles on actin cables demonstrate an unexpected rapid cycle of formin activation at the cell tip and release from the cell tip.

Results

The Formin For3p Displays Rapid Movements Away from Cell Tips

We imaged the formin for3p in living cells by using a *for3-3GFP* construct that was expressed under the endogenous promoter at the *for3* chromosomal locus, replacing the endogenous *for3*$^{+}$ gene. This construct was fully functional, as demonstrated by normal cell morphology and assembly of actin cables (Figure S1 available in the Supplemental Data with this article online). We observed that for3p-3GFP resided in small dots enriched at cell tips in interphase cells (Figures 1A and 1B). In dividing cells, in which actin cables emanate from the cell division site [17], for3p-3GFP dots concentrated at the cell division site. Time-lapse imaging revealed that for3p particles were extremely dynamic. For3p-3GFP dots remained at cell tips for only a few seconds before either disappearing or detaching from the cortex and moving inward. The majority of dots that could be followed over several timeframes showed a linear movement away from cell tips into the center of the cell (Figures 1A and 1B and Movie S1). Dots often appeared to follow each other in well-defined tracks. For3p-3GFP dots moved away from the cell tips at a rate of 0.33 ± 0.11 μm/s (n = 126 dots in 62 cells), as measured by using kymographs (Figures 1A–1C). In dividing cells, for3p-3GFP dots moved with similar rates away from the cell division site. The rate of individual for3p dots was constant, although in rare instances we observed changes in the rate of movement of a single dot. We also occasionally detected for3p dots moving in the opposite direction, toward cell tips, and this movement generally occurred at the significantly higher

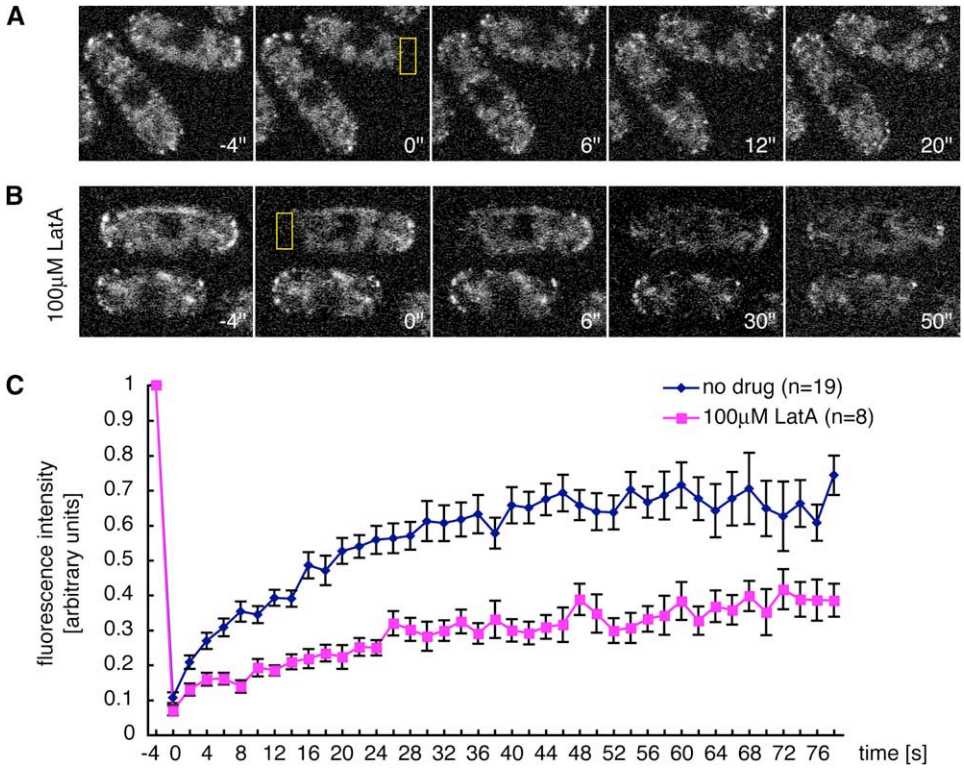

Figure 2. FRAP Analysis of For3p Dynamics

(A and B) Cells expressing for3p-3GFP were photo-bleached in the boxed regions and then imaged over time by using a laser scanning confocal microscope. The boxed regions, which contain 10%–30% of total cellular fluorescence, were photo-bleached at time 0. Note the longer recovery time for cells treated with 100 μM LatA (bottom row).

(C) Quantification of the fluorescence intensity recovery. Each trace represents the average value for the indicated number of experiments. Error bars show the standard error of the mean.

rate of 0.98 ± 0.46 μm/s (n = 19 in 14 cells) (Figures 1B and 1C). It is unclear whether these movements toward cell tips occur less frequently or whether their fast rate simply renders their detection more difficult.

The exact composition of these for3p-3GFP dots is not yet known. Formins form dimers in solution [6, 25]. Measurements of for3p-3GFP fluorescence intensities suggested that noncortical dots contain small numbers of for3p molecules (average = 4.2 ± 1.7, range 1–10, and n = 30; see Experimental Procedures).

As an independent measure of for3p dynamics, we performed FRAP experiments in which we photo-bleached for3p-3GFP at one tip of a single cell and measured the recovery of fluorescence over time (Figures 2A and 2C). The average $t_{1/2}$ of recovery was ~10 s. In individual FRAP experiments, there was considerable variability of fluorescence intensities within the bleached zone between consecutive time points, probably due to the movement of individual for3p particles. These FRAP studies showed that most, and possibly all, for3p was dynamic at cell tips. These data suggest that, on average, the population of for3p at the cell tip exchanges about every 20 s.

To understand the mechanism of for3p movements, we examined the possible roles of F-actin, microtubules, and membrane trafficking. Depolymerization of microtubules (with methyl-benzidazole-carbamate [MBC]) or disruption of membrane trafficking (with brefeldin A) had no effect on for3p-3GFP behavior (data not shown). In contrast, all for3p-3GFP movements were abolished by treatment with 100 μM Latrunculin A (LatA) (Figure 1D and Movie S2). LatA binds actin monomers and effectively decreases the pool of polymerization-competent monomers [26]. At such high doses, LatA inhibits actin polymerization and causes the rapid loss of all F-actin structures. In these cells, for3p-3GFP was concentrated as dots at the cell tip, with no distinct dots present in other cytoplasmic regions. Similar results were noted previously by using the for3p-YFP fusion [16]. FRAP experiments showed that the turnover of for3p-3GFP at the cell tip was significantly reduced in cells treated with 100μM LatA (Figures 2B and 2C). Residual turnover in LatA-treated cells may be due to residual (though undetectable) actin, as an actin binding mutant of for3p had no detectable turnover (see Figure 5E). Assuming a steady-state situation, in which for3p arrives and binds to saturable cortical sites and then leaves these sites at equal rates, the turnover measured by FRAP can be affected by conditions that affect departure as well as delivery to these sites. As the delivery and binding of for3p to cortical docking sites appears to be largely independent of actin (Figure 1D), this decrease in turnover in LatA-treated cells may reflect a reduced rate of for3p departure from the cell tip. Thus, these findings, together with the observations of actin-dependent for3p movements

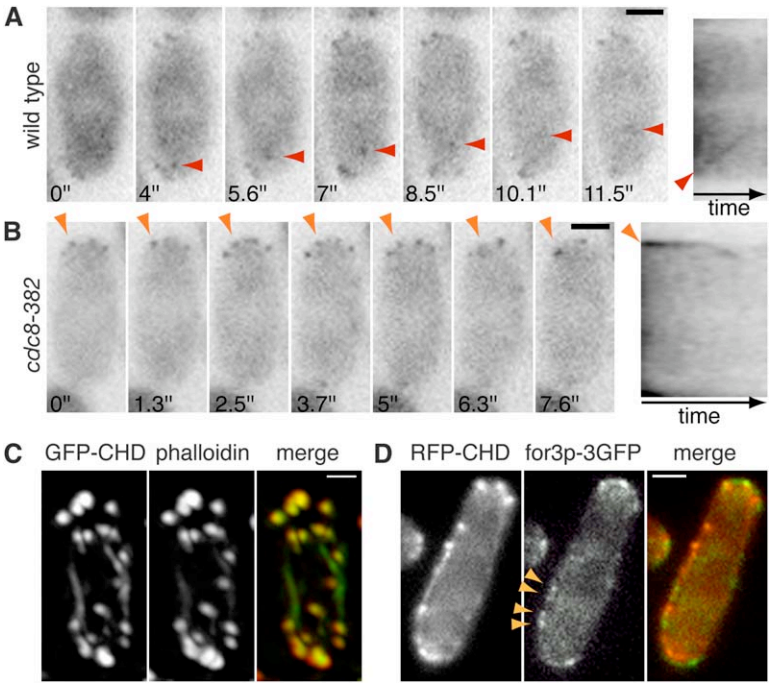

Figure 3. For3p Moves on Actin Cables

(A and B) Time-lapse images and corresponding kymographs of for3p-3GFP in wild-type (A) and tropomyosin mutant (*cdc8-382*; [B]) at 36°C. Only very short movements were observed in the tropomyosin mutant.

(C) GFP-CHD_{rng2} (green in the merge image) colocalizes with actin patches and cables stained with rhodamine-phalloidin (red).

(D) For3p-3GFP (green in the merge image) localizes on RFP-CHD_{rng2}-labeled actin cables (red) but does not colocalize with actin patches (bright foci labeled by RFP-CHD_{rng2}).

away from cell tips, suggest that actin contributes to for3p dynamics primarily by moving for3p away from cortical binding sites at the cell tip.

For3p Moves on Actin Cables

We next tested whether for3p-3GFP dots move on actin cables. Low dose of LatA (1 μM), which leads to loss of actin cables, but not actin patches, in almost all cells, resulted in accumulation of for3p at the cell cortex and abolished for3p movements completely in most cells (data not shown). In *cdc8-382* tropomyosin mutant cells, which lack actin cables, but not patches [19, 27], for3p exhibited no long-range movements but rather appeared to be stable at cell tips for longer periods of time and displayed only short inward movements before disappearing (Figure 3B). Under similar conditions, long-range linear movements were observed in the wild-type strain (Figure 3A). Thus, for3p movements require actin cables.

We next directly imaged for3p-3GFP dots with actin cables. We visualized actin cables in live cells by using fusion proteins between the calponin-homology domain (CHD) of the IQGAP-like protein rng2p and GFP or RFP, which were expressed from an inducible promoter [28]. Costaining of GFP-CHD_{rng2} expressing cells with rhodamine phalloidin confirmed that this construct labels all actin structures in the cell (Figure 3C). Time-lapse dual imaging of RFP-CHD_{rng2} and for3p-3GFP revealed that for3p dots localize to and move along actin cables (Figure 3D and Movie S3). In addition, for3p dots did not colocalize with actin patches. Thus, for3p moves away from the cell tips on actin cables.

For3p Movements Depend on Actin Polymerization

To determine the mechanism of for3p movement, we next examined the possible roles of actin motor proteins and actin polymerization machinery. In mutants for myosin type I (*myo1*Δ), type II (*myo2-E1* and *myp2*Δ), and type V (*myo51*Δ and *myo52*Δ), for3p movements were still present, indicating that none of these barbed-end-directed myosins were essential for for3p movements (data not shown). *S. pombe* has no predicted pointed-end-directed myosins. However, preliminary observations suggest that myosin V may contribute to for3p movement outwards toward cell tips (S.G.M., unpublished data).

Formin movements were dependent on actin polymerization. To vary the rate of actin filament polymerization in vivo, we treated cells with low concentrations of LatA to decrease the pool of polymerization-competent monomers. Analysis of for3p dot movements in increasing concentration of LatA up to 1μM revealed a linear dose-dependent reduction in speed (Figure 4A). This suggests that actin polymerization may directly drive movement. Formin movement was not affected in mutants of the Arp2/3 actin polymerization machinery (mutants in arp2p and its activators myo1p and wsp1p; Table S1 and data not shown). Thus, the mechanism of for3p movements occurs through an actin-polymerization-based mechanism, distinct from motor or Arp2/3-based motility.

Bulk Actin Cable Elongation Occurs at the Same Rate as For3p Movements

To compare the rate of actin cable elongation with the rate of for3p movement, we imaged actin cable dynamics in cells expressing the GFP-CHD_{rng2} reporter. Actin cables were largely oriented along the long axis of the cell, usually enriched along the cortex, and displayed a number of dynamic behaviors, including growth, shrinkage, and occasionally fusion (Movie S4). The fluorescence intensities along a cable were not uniform, suggesting uneven packing of actin filaments within the cable. Marks on actin cables moved away from the

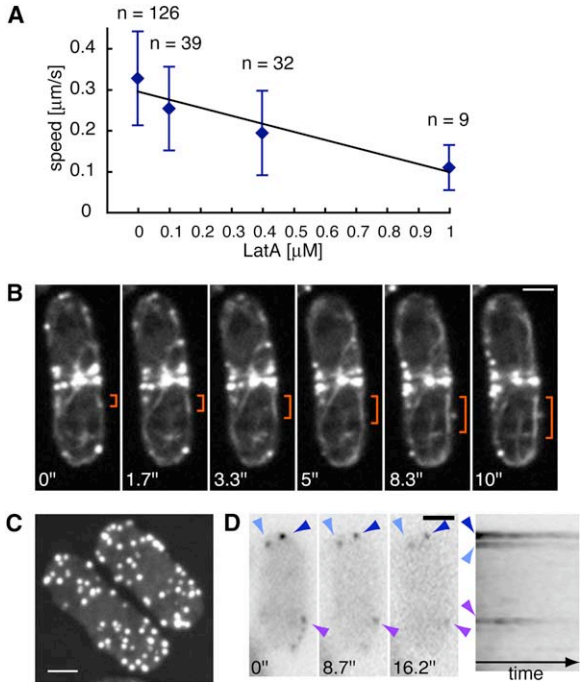

Figure 4. For3p Movements Correlate with Actin Polymerization Rates

(A) The effect of LatA concentration on the rate of for3p-3GFP movement. Note that the rate at 1 μM LatA is probably an overestimate, as static dots at cell tips were not included in the analysis. Error bars show the standard deviation.

(B) Time-lapse images of actin cables in a dividing cell expressing an actin marker, GFP-CHD_{mg2}. During this cell cycle phase, cables are assembled from the medial region in a for3p-dependent manner. A region of brighter intensity, which may represent an actin filament growing out from the cell center of this dividing cell, is indicated by the orange bracket. Scale bar represents 2 μm.

(C) Profilin mutant cells (*cdc3-313*) grown at 36°C for 30 min and stained with AlexaFluor 488-phalloidin, showing the absence of actin cables.

(D) Time-lapse images and corresponding kymographs of for3p-3GFP in a profilin mutant (*cdc3-313*) at 36°C. For3p dots are static.

cell tip. This pattern was largely consistent with the bulk of actin polymerization occurring at the cell tip, resulting in bulk movement of actin filaments away from the cell tip, similar to retrograde actin flow. These movements were consistent with EM studies and confirm that the growing barbed ends are oriented toward cell tips in interphase and toward the cell center in dividing cells [17]. The marks on cables moved away from the cell tip at a rate very similar to for3p-3GFP movements: 0.30 ± 0.06 μm/s (n = 30) (Figure 4B and Movie S5). Actin cable marks move with similar rates in budding yeast, where similar measurements have been used to evaluate actin cable elongation [29]. Notably, in the presence of 0.4 μM LatA, actin cables exhibited marks that moved at the significantly lower rate of 0.22 ± 0.09 μm/s (n = 11), similar to reduced rates of for3p dots of 0.19 ± 0.10 μm/s. One caveat of this approach is that it is not possible to rule out that some of the movements represent not bulk movement of the whole cable but rather sliding of individual filaments within a cable. Unfortunately, the use of photo-bleaching to generate fiduciary marks on the actin cable was not technically feasible. These data do suggest, however, that the rate of formin movements matches the retrograde movement of bulk actin flow in the actin cable both in wild-type cells and in cells treated with low dose of LatA.

For3p Associates with Actin Cables via the FH2 Domain

For3p could bind to the actin cable by remaining on the barbed end of actin filaments or, alternatively, by binding to other sites on the actin filament or to another actin binding protein. To test these possibilities, we generated a point mutation in the conserved actin binding region of the FH2 domain (I930A) involved in barbed end association [25]. This mutant for3p protein is predicted to be defective in nucleation and interaction with the barbed end of actin filaments but is likely to still dimerize, as mutant and wild-type for3p coexpressed in the same cell coimmunoprecipitate (data not shown). In cells that expressed 3GFP-tagged for3p-I930A as its only for3p protein, actin cables were absent (Figure 5A). Not surprisingly, as in other mutants lacking actin cables, the mutant formin accumulated at the cell tip and did not exhibit any detectable movements (Figure 5B and Movie S6).

Next, we created a situation in which we could follow the behavior of the formin mutant protein in a cell containing actin cables. We expressed wild-type for3p from a plasmid in cells containing chromosomal 3GFP-tagged for3p-I930A. In these cells, for3p-I930A-3GFP accumulated at the cell tip, but no dots moved away from the cell tip even in the presence of actin cables (Figures 5C and 5D and Movie S7). Thus, consistent with the LatA results (Figure 1D), this actin interaction domain of for3p is required for association with actin cables, but not for cortical docking.

FRAP studies of wild-type for3p and for3p-I930A in the presence or absence of actin cables were consistent with the time-lapse imaging (Figure 5E). The *for3-I930A* mutant was largely immobile at the cortex in the absence of actin cables. In cells expressing for3p-I930A-3GFP and wild-type for3p, there was a clear decrease in turnover compared to that in cells expressing wild-type for3p-3GFP and wild-type for3p. Thus, the for3p-I930A mutant has a defect in turnover even in the presence of actin cables, which probably reflects the fact that the mutant for3p does not efficiently leave the cell tip. Thus, these data suggest that for3p needs to bind to the barbed end of the actin filament to leave the cell tip and travel down the actin cable.

For3p Movements Depend on Profilin and Bud6p, but Not Tea4p or Rho3p

The quantification of for3p movements on the actin cable can provide an assay of for3p activity in vivo. We examined the role of four formin-interacting proteins. Profilin, a G-actin binding protein, may bind directly to the proline-rich sites in the formin FH1 domain and stimulates formin activity in vitro [30, 31]. A conditional profilin mutant (*cdc3-313*) exhibited no actin cables and no for3p movement, suggesting that profilin is necessary for for3p activity in vivo (Figures 4C and 4D).

Tea4p binds to the N-terminal region of for3p and recruits for3p to one of the cell ends to establish bipolar growth [20]. Overexpression of tea4p leads to a large accumulation of actin cables and thus has been suspected

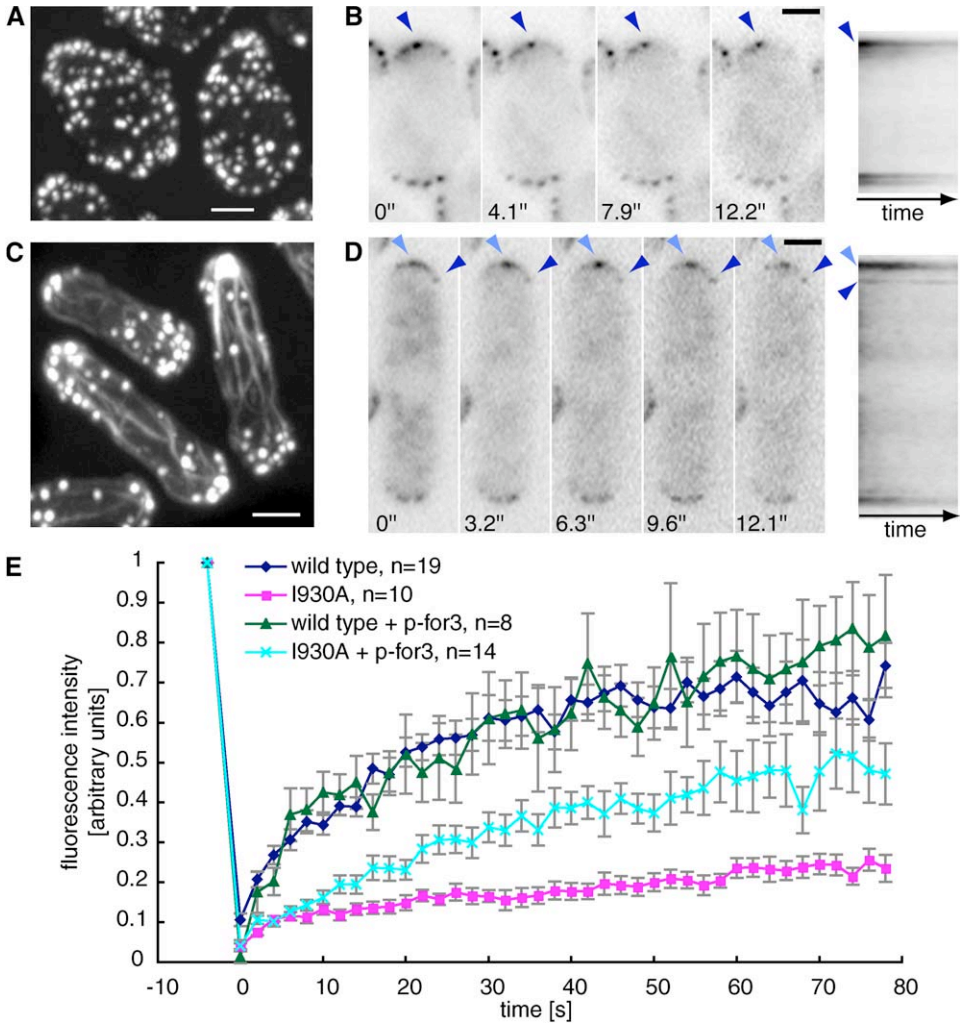

Figure 5. For3p Movements Depend on Actin Binding within the FH2 Domain

(A) *for3-I930A-3GFP* mutant cells stained with AlexaFluor 488-phalloidin, showing the absence of actin cables.

(B) Time-lapse images and corresponding kymograph of for3p-I930A-3GFP are shown. All for3p dots are static at the cell tips.

(C) *for3-I930A-3GFP* mutant cells expressing untagged wild-type for3p and stained with AlexaFluor 488-phalloidin, showing normal morphology and presence of actin cables.

(D) Time-lapse images and corresponding kymograph of for3p-I930A-3GFP expressing untagged wild-type for3p. Despite the presence of actin cables, for3p dots remain static at the cell tips.

(E) FRAP analysis of wild-type for3p-3GFP and mutant for3p-I930A-3GFP fluorescence in the presence or absence of untagged plasmid expressing wild-type for3p (p-for3). Each trace represents the average value for the indicated number of experiments. Error bars show the standard error of the mean.

of stimulating for3p activity [20]. However, in *tea4*Δ cells, for3p-3GFP movements at the one growing cell tip were not significantly different from wild-type (Table S1). Thus, although tea4p is needed for establishment of for3p at a new end, at preexisting sites of growth at the old end, it does not contribute significantly to formin activity. Rho3p also binds the N-terminal region of for3p, but the role of this interaction is unclear [15]. In *rho3*Δ cells, for3p-3GFP behavior was not significantly different from wild-type (Table S1), suggesting that rho3p is not essential for for3p activation.

Bud6p binds to the C-terminal region of for3p [21] and is a homolog of *S. cerevisiae* Bud6p, which is an actin-monomer binding protein that stimulates formin activity in vitro [6]. In *S. pombe bud6*Δ mutants, cables are present but thinner [21]. In these cells, for3p-3GFP dots were less distinct and exhibited centripetal movements at a rate of 0.25 ± 0.14 μm/s (n = 70), a rate significantly slower than wild-type (t test, $p < 0.005$). Thus, profilin and bud6p contribute to the rate of formin-driven actin polymerization in vivo.

For3p Releases from Bud6p

We next examined whether for3p travels on the actin cable by itself or moves associated with other proteins in the formin complex such as bud6p. Using a functional bud6p-RFP (a tomato-dimer variant [32]) fusion construct, we coimaged bud6p and for3p. As observed previously [21, 33], bud6p dots partially colocalized with for3p dots at the cell tip (Figure 6A). In LatA-treated cells, the colocalization of for3p and bud6p dots was more precise (Figure 6B). Time-lapse imaging revealed

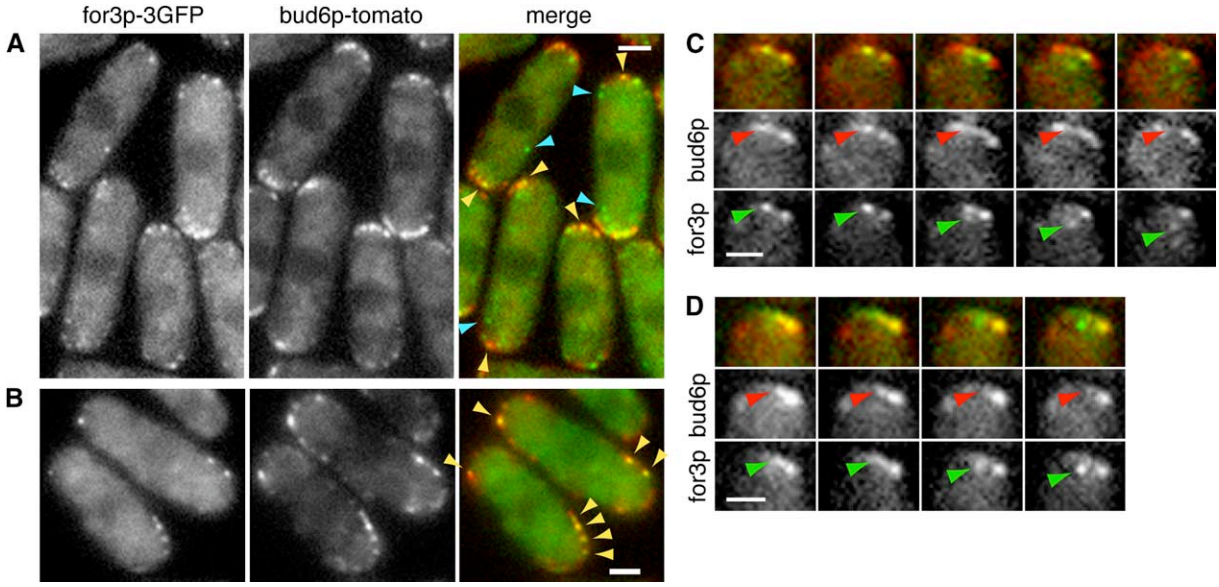

Figure 6. For3p Associates Transiently with Bud6p at Cell Tips

(A) Simultaneous two-color image of for3p-3GFP (green in the merge image) and bud6p-RFP tomato (red). For3p and bud6p colocalize partially at cell tips (shown with yellow arrowheads), but bud6p is absent from for3p dots (blue arrowheads) in the cell interior.

(B) Two-color image of for3p-3GFP (green in the merge image) and bud6p-tomato (red) treated with 100 μM LatA for 30 min. Although long treatment with LatA leads to delocalization of both proteins, all cortical for3p dots at the cortex colocalizes with bud6p (highlighted with yellow arrowheads).

(C and D) Two-color time-lapse images of for3-3GFP (green in the merge image) and bud6p-RFP tomato (red) a cell tip. Images were taken every 600 ms. Panels show a for3p dot on the cortex that moves into the cell interior (green arrowheads), while bud6p remains at the cortex and decreases in intensity (red arrowheads).

that for3p and bud6p started off in the same place at the cell tip, but when for3p dots detached from the cell tip and moved into the cell interior, bud6p did not move with for3p. Rather, bud6p was left behind at the cortex and often decreased in intensity (Figures 6C and 6D and Movie S8). To test whether the bud6p-RFP construct was simply not bright enough, we further observed that a functional bud6p-3GFP fusion expressed under the endogenous promoter also stayed at the cell tips and did not exhibit any movements into the cell (Movie S9). Thus, for3p may associate only transiently with its activator bud6p at the cortex.

Discussion

Taken together, the data presented here provide a new model in which for3p participates in a dynamic cycle for actin cable assembly (Figure 7): formin proteins bind transiently to the cortex, perhaps via a docking complex at the cell tip. During this period, the formin is activated and nucleates a short actin filament. The filament grows at a rate of 0.3 μm/s, which corresponds to addition of about 100 actin subunits per second. The actin filament is bundled into the cable through actin crosslinking proteins: formins themselves may also participate in bundling [34, 35]. After ~20 s at the cortex, the formin and its associated barbed end are then released. The filaments in the cable are pushed into the cell interior by polymerization of the actin filaments driven by active formins at the cortex. We imagine that in some cases, upon release from the cortex, the formin remains bound to the barbed end, so that it is carried into the cell with its associated actin filament by retrograde actin "flow." As cables have a limited length, there must ultimately be disassembly of the cable and consequent release of the formin from the cable. Finally, for3p may be carried back to the cell tip by either diffusion or active transport. This for3p cycle may serve as an inherent part of a mechanism for how short actin filaments are continuously assembled in the actin cable.

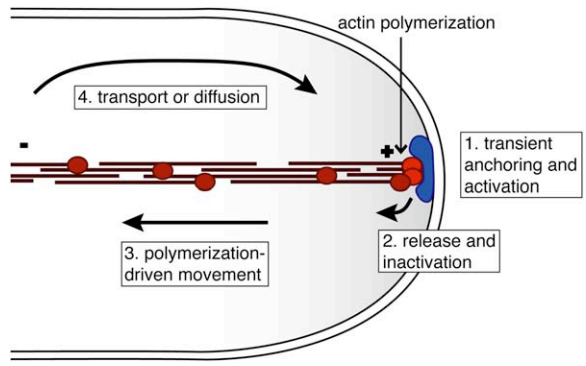

Figure 7. Model for For3p Regulation and Actin Cable Assembly In Vivo

For3p particles (red circles) may represent formin dimers or larger oligomers. These formin particles are transiently anchored and activated at the cell tip, where they assemble a short actin filament that is incorporated into the actin bundle. For3p is then released and occasionally remains bound to the barbed end of the actin filament, probably in an inactive state. As the actin filaments in the bundle are moved by the polymerization of actin from the active formins at the cell tip, these inactive for3p particles on the actin barbed end are also moved away from the cell tip. After disassociation of for3p and/or disassembly of the cable, for3p may then return to the cell tip by active transport or diffusion.

These studies suggest the existence of a docking complex at the cell tip that transiently recruits, activates, and then releases for3p for the process of actin cable assembly. Components of this "machine" may include for3p-interacting proteins, such as tea4p, bud6p, rho3p, and cdc42p. However, no mutant has been found to have complete loss of for3p localization [15, 20, 21]. It is therefore likely that multiple factors contribute to the proper docking and regulation of this formin. Turnover of the formin within the complex is likely to be governed by several factors, including delivery and actin cable-dependent release. The arrival of for3p to this docking complex may occur by both actin-dependent and actin-independent movements. We have noted occasional for3p dots that move in a directional manner toward cell tips in an actin-cable-dependent manner, at rapid rates consistent for myosin V-driven transport. However, it is unlikely that delivery on actin cables is the sole mechanism, as the number of for3p particles moving to the cell tip is small, and actin cables are not required (at least in the short term) for for3p targeting. Rather, it is likely that free diffusion contributes to for3p delivery, as a portion of for3p appears to be in a free cytoplasmic pool, visualized as a diffuse haze.

In addition to localization, the activity of formin must also be regulated during this cycle: we speculate that for3p promotes actin nucleation or elongation transiently at the cell tip and then may become inactive when it moves into the cell interior. Our observations suggest that formins on the cable are not continuously promoting assembly. For instance, for3p appears to associate with its activator bud6p only at the cell cortex. Actin cables do not get progressively thicker away from cell tips. Formins may be inactivated when they are released from the cortex but still retain the ability to bind to the filament barbed end, where that could contribute to capping activity. Thus, the spatial control of for3p activation may ensure the appropriate organization and polarity of actin cables.

Like the lamella [36], the actin cable is an attractive system to study the mechanism of actin assembly, as the different steps can be visualized with spatial and temporal resolution. Despite the contrasting mechanisms of action of formins and arp2/3 nucleators, the results presented here suggest similarities between the two systems. Arp2/3 activators associate only transiently with Arp2/3 at the cell cortex [37], which then remains bound to the actin network and moves away from the cortex with actin retrograde flow. Similarly, we have shown here that the formin for3p integrates into the actin structures it assembles and associates only transiently with its activator bud6p at the cell cortex, suggesting a defined temporal order of events. The rapid dynamics of this system may facilitate accurate spatial regulation of formin activation and allow for quick remodeling of the actin cytoskeleton in response to various signals and polarization cues.

Experimental Procedures

Yeast Strains, Plasmids, and Biochemical Methods

S. pombe strains used in this study are listed in Table S2. Standard methods for *S. pombe* media, genetic manipulations, and molecular biology were used throughout. All plasmids were sequenced.

For for3-3GFP tagging, *ura4*$^{+}$ amplified with primers osm451 (5′-AGCTCTAGAAAGCTTGTGATATTGACGAAAC-3′) and osm452 (5′-AGCTCTAGAAAGCTTAGCTACAAATCCCAC-3′) was introduced in the XbaI site of pRS304-3xGFP (kindly provided by D. Pellman) to yield pSM458 (restriction sites underlined). A composite fragment consisting of 500 bp of the *for3* 3′UTR, a PstI site, and 500 bp of the end of the *for3* ORF was then inserted upstream of the 3GFP cassette to create pSM461. Genomic integration was obtained by transformation of pSM461 linearized with PstI and verified by PCR and Western blotting.

For for3-I930A point mutant, I930 was identified by sequence comparison to correspond to I1431 in *S. cerevisiae* Bni1p [25]. The I930A mutation was created by site-directed mutagenesis on a plasmid coding for for3$_{(630–1461)}$. In a wild-type strain, the genomic *for3* FH2 region was replaced with *ura4*$^{+}$ to yield strain YSM588, which was transformed with a linearized for3$_{(630–1461)}$(I930A) fragment. *ura4*$^{-}$ colonies were selected on 5-fluoroorotic acid, and integration was confirmed by PCR.

To create the RFP-CHD$_{rng2}$ plasmid, RFP amplified from pDsRed1.M1-N1 (provided by B. Glick) with primers osm569 (5′-GAAGTCGACATGGACAACACCGAGGACGTC-3′) and osm570 (5′-GAACTCGAGGCCTGGGAGCCGGAGTGGCGGG-3′) was digested with SalI/XhoI and cloned into pREP41x digested with XhoI to yield pSM526. A SalI-SacI CHD$_{rng2}$-containing fragment from pREP42-GFP-CHD$_{rng2}$ (pCDL270; a gift from M. Balasubramanian) was subcloned into pSM526 cut with XhoI-SacI to obtain pSM528.

Complementation of for3p function in *for3-I930A* mutant was performed with pREP3x-for3 cultured in the presence of thiamine (repressed condition).

For bud6p tagging, a PCR-based method was used with pFA6a-3GFP-kanMX and pFA6a-RFP (tomato dimer)-natMX as templates (gifts from T. Pollard and K. Sawin, respectively) [33].

To test for for3p dimerization, wild-type, *for3-3GFP*, and *for3-I930A-3GFP* strains transformed with pREP3x-HA-for3 were grown in the presence of thiamine. Coimmunoprecipitations with an anti-GFP antibody were performed as described [20].

Microscopy and Pharmacological Inhibitors

For quantification of cable dynamics, single focal plane time-lapse images were acquired with 700 ms exposure using a spinning disk confocal microscope (Nikon E600 upright microscope fitted with a Yokogawa CSU-10 spinning disk confocal unit, a Plan Apo x100/1.4 objective, and a Hamamatsu ORCA-ER cooled CCD camera). For all other time-lapse imaging, a wide-field fluorescence microscope (Nikon E800 upright microscope equipped with a Plan Apo x 100/1.4 objective and a Hamamatsu C4742-95 cooled CCD camera) was used. For two-color live imaging, red and green channels were collected simultaneously by using a Dual View image splitter on a wide-field microscope [38]. For3p-3GFP images were acquired in single focal planes with 500 ms exposure, processed, and analyzed with the OpenLab software (Improvision). For figure preparation, images were transferred to Adobe Photoshop and their size was doubled by using the default bicubic resampling tool. FRAP experiments were performed on a laser scanning confocal microscope (Zeiss LSM 510 Meta). Photo-bleaching was obtained by 25 iterative scans of a selected region encompassing the very tip of a cell at maximal laser power. Images were recorded before photo-bleaching, immediately after, and subsequently every 2 s, with 5% laser power.

To prepare cells for imaging, for3p-3GFP strains were grown in Edinburgh minimal media supplemented with appropriate amino acids (EMM-AUL) overnight at 30ºC to log phase and observed at room temperature (22ºC –24ºC), unless otherwise noted. Temperature-sensitive mutants were grown at 25ºC, shifted to 36ºC for 40 min, and imaged with an objective heater (Bioptechs, Butler, Pennsylvania) at 36ºC. To image live actin cables, GFP- (or RFP-) CHD$_{rng2}$ expression was induced for 16 hr in medium lacking thiamine. Actin staining was performed as described by using AlexaFluor 488-phalloidin (Molecular Probes). For costaining of GFP-CHD$_{rng2}$ and rhodamine-phalloidin, cells were permeabilized on a microscope slide with 1% Triton X-100 in the presence of 1M sorbitol, stained with rhodamine-phalloidin, and imaged immediately. 100× stock solutions of LatA (provided by P. Cruz, UC Santa Cruz) were prepared in dimethylsulfoxide (DMSO). Negative controls included addition

of 1% DMSO alone, which had no influence on the movements of for3p.

Image Data Analysis

For3p-3GFP movements were analyzed with kymographs, which were constructed with the "Volume Slicing" tool of the OpenLab software. The velocity of individual dots was extracted from the length (l) of their trace in the kymograph and its angle (α) with the vertical (velocity = d/t, where d = sin[α]*l and t = cos[α]*l). Measurements of cable dynamics were performed by recording the (x, y) position of growing cable ends or internal fiduciary marks over at least four consecutive time points. The rate of movement was calculated as the sum of the distances between the points divided by time.

For analysis of the FRAP experiments, the mean fluorescence intensities were measured over time in three regions: (1) the photobleached region, (2) the background, and (3) another nonbleached cell. For each time point, the intensities of the bleached region and of the unrelated cell were adjusted by subtracting background signal. To correct for loss of signal due to imaging, the adjusted bleached region intensity was then divided by the adjusted intensity of the other cell. For each experiment, all values were normalized so that the prephoto-bleaching value equals 1. Finally, averages and standard errors were derived for fluorescence values at individual time points.

To estimate the number of for3p molecules, we quantified the average fluorescence intensity of whole cells in wide-field images (single focal plane) of for3p-3GFP and compared it to cdc12p-3GFP (A. Yonetani and F.C., unpublished data). After subtraction of background values (camera background as well as fluorescence intensity of cells that did not express GFP), we found that the total for3p-3GFP signal was about 3× higher than that of cdc12p-3GFP, giving an estimated 1800 molecules of for3p per cell (Wu and Pollard [2005] had previously measured an approximate concentration of cdc12p-3YFP of 600 molecules per cell [39]). Similar for3p numbers were derived in ratios with cdc7-GFP fluorescence [39]. To quantify the fluorescence intensity of individual for3p-3GFP dots, we measured the average fluorescence intensity of a 3 × 3 pixel square surrounding the dot. We also measured the average fluorescence intensity of a 2-pixel-wide rim around this square—this value gave an approximate local measure of diffuse for3p. After subtraction of background values, this second value was subtracted from the first, which gave us the estimated average intensity of the dot. We then calculated what percentage of total cell fluorescence was present in the dot, which varied between 0.07%–0.5%, which represents an average of about four for3p molecules/dot (range 1–10). We emphasize that these measurements need to be taken with caution, given that the numbers are derived from multiple measurements, each with its own level of uncertainty.

Supplemental Data

Supplemental Data include one figure, two tables, and nine movies and can be found with this article online at http://www.current-biology.com/cgi/content/full/16/12/1161/DC1/.

Acknowledgments

We wish to thank M. Balasubramanian, B. Glick, D. Pellman, T. Pollard, K. Sawin, and A. Yonetani for reagents, S. Yoshida and D. Pellman for sharing unpublished data and discussions, L. Pon and T. Huckaba for use of their Dual View image splitter imaging system, the Columbia University Medical Center confocal facility for assistance in FRAP studies, and R. Benton and members of the Chang lab for critically reading the manuscript and useful discussions. This work was supported by a Human Frontier Science Program Organization long-term fellowship to S.G.M. and National Institutes of Health GM056836 to F.C.

Received: March 3, 2006
Revised: April 7, 2006
Accepted: April 24, 2006
Published: June 19, 2006

References

1. Wallar, B.J., and Alberts, A.S. (2003). The formins: active scaffolds that remodel the cytoskeleton. Trends Cell Biol. *13*, 435–446.
2. Pruyne, D., Evangelista, M., Yang, C., Bi, E., Zigmond, S., Bretscher, A., and Boone, C. (2002). Role of formins in actin assembly: nucleation and barbed-end association. Science *297*, 612–615.
3. Sagot, I., Rodal, A.A., Moseley, J., Goode, B.L., and Pellman, D. (2002). An actin nucleation mechanism mediated by Bni1 and profilin. Nat. Cell Biol. *4*, 626–631.
4. Zigmond, S.H., Evangelista, M., Boone, C., Yang, C., Dar, A.C., Sicheri, F., Forkey, J., and Pring, M. (2003). Formin leaky cap allows elongation in the presence of tight capping proteins. Curr. Biol. *13*, 1820–1823.
5. Harris, E.S., Li, F., and Higgs, H.N. (2004). The mouse formin, FRLalpha, slows actin filament barbed end elongation, competes with capping protein, accelerates polymerization from monomers, and severs filaments. J. Biol. Chem. *279*, 20076–20087.
6. Moseley, J.B., Sagot, I., Manning, A.L., Xu, Y., Eck, M.J., Pellman, D., and Goode, B.L. (2004). A conserved mechanism for Bni1- and mDia1-induced actin assembly and dual regulation of Bni1 by Bud6 and profilin. Mol. Biol. Cell *15*, 896–907.
7. Romero, S., Le Clainche, C., Didry, D., Egile, C., Pantaloni, D., and Carlier, M.F. (2004). Formin is a processive motor that requires profilin to accelerate actin assembly and associated ATP hydrolysis. Cell *119*, 419–429.
8. Kovar, D.R., Kuhn, J.R., Tichy, A.L., and Pollard, T.D. (2003). The fission yeast cytokinesis formin Cdc12p is a barbed end actin filament capping protein gated by profilin. J. Cell Biol. *161*, 875–887.
9. Kovar, D.R., Harris, E.S., Mahaffy, R., Higgs, H.N., and Pollard, T.D. (2006). Control of the assembly of ATP- and ADP-actin by formins and profilin. Cell *124*, 423–435.
10. Kovar, D.R., and Pollard, T.D. (2004). Insertional assembly of actin filament barbed ends in association with formins produces piconewton forces. Proc. Natl. Acad. Sci. USA *101*, 14725–14730.
11. Higashida, C., Miyoshi, T., Fujita, A., Oceguera-Yanez, F., Monypenny, J., Andou, Y., Narumiya, S., and Watanabe, N. (2004). Actin polymerization-driven molecular movement of mDia1 in living cells. Science *303*, 2007–2010.
12. Li, F., and Higgs, H.N. (2003). The mouse Formin mDia1 is a potent actin nucleation factor regulated by autoinhibition. Curr. Biol. *13*, 1335–1340.
13. Alberts, A.S. (2001). Identification of a carboxyl-terminal diaphanous-related formin homology protein autoregulatory domain. J. Biol. Chem. *276*, 2824–2830.
14. Watanabe, N., Kato, T., Fujita, A., Ishizaki, T., and Narumiya, S. (1999). Cooperation between mDia1 and ROCK in Rho-induced actin reorganization. Nat. Cell Biol. *1*, 136–143.
15. Nakano, K., Imai, J., Arai, R., Toh, E.A., Matsui, Y., and Mabuchi, I. (2002). The small GTPase Rho3 and the diaphanous/formin For3 function in polarized cell growth in fission yeast. J. Cell Sci. *115*, 4629–4639.
16. Feierbach, B., and Chang, F. (2001). Roles of the fission yeast formin for3p in cell polarity, actin cable formation and symmetric cell division. Curr. Biol. *11*, 1656–1665.
17. Kamasaki, T., Arai, R., Osumi, M., and Mabuchi, I. (2005). Directionality of F-actin cables changes during the fission yeast cell cycle. Nat. Cell Biol. *7*, 916–917.
18. Motegi, F., Arai, R., and Mabuchi, I. (2001). Identification of two type V myosins in fission yeast, one of which functions in polarized cell growth and moves rapidly in the cell. Mol. Biol. Cell *12*, 1367–1380.
19. Pelham, R.J., Jr., and Chang, F. (2001). Role of actin polymerization and actin cables in actin-patch movement in Schizosaccharomyces pombe. Nat. Cell Biol. *3*, 235–244.
20. Martin, S.G., McDonald, W.H., Yates, J.R., 3rd, and Chang, F. (2005). Tea4p links microtubule plus ends with the formin for3p in the establishment of cell polarity. Dev. Cell *8*, 479–491.

21. Feierbach, B., Verde, F., and Chang, F. (2004). Regulation of a formin complex by the microtubule plus end protein tea1p. J. Cell Biol. *165*, 697–707.
22. Higgs, H.N., and Peterson, K.J. (2004). Phylogenetic analysis of the formin homology 2 domain. Mol. Biol. Cell *16*, 1–13.
23. Pruyne, D., Gao, L., Bi, E., and Bretscher, A. (2004). Stable and dynamic axes of polarity use distinct formin isoforms in budding yeast. Mol. Biol. Cell *15*, 4971–4989.
24. Ozaki-Kuroda, K., Yamamoto, Y., Nohara, H., Kinoshita, M., Fujiwara, T., Irie, K., and Takai, Y. (2001). Dynamic localization and function of Bni1p at the sites of directed growth in Saccharomyces cerevisiae. Mol. Cell. Biol. *21*, 827–839.
25. Xu, Y., Moseley, J.B., Sagot, I., Poy, F., Pellman, D., Goode, B.L., and Eck, M.J. (2004). Crystal structures of a Formin Homology-2 domain reveal a tethered dimer architecture. Cell *116*, 711–723.
26. Coue, M., Brenner, S.L., Spector, I., and Korn, E.D. (1987). Inhibition of actin polymerization by latrunculin A. FEBS Lett. *213*, 316–318.
27. Arai, R., Nakano, K., and Mabuchi, I. (1998). Subcellular localization and possible function of actin, tropomyosin and actin-related protein 3 (Arp3) in the fission yeast Schizosaccharomyces pombe. Eur. J. Cell Biol. *76*, 288–295.
28. Karagiannis, J., Bimbo, A., Rajagopalan, S., Liu, J., and Balasubramanian, M.K. (2005). The nuclear kinase Lsk1p positively regulates the septation initiation network and promotes the successful completion of cytokinesis in response to perturbation of the actomyosin ring in Schizosaccharomyces pombe. Mol. Biol. Cell *16*, 358–371.
29. Yang, H.C., and Pon, L.A. (2002). Actin cable dynamics in budding yeast. Proc. Natl. Acad. Sci. USA *99*, 751–756.
30. Kovar, D.R. (2006). Molecular details of formin-mediated actin assembly. Curr. Opin. Cell Biol. *18*, 11–17.
31. Chang, F., Drubin, D., and Nurse, P. (1997). cdc12p, a protein required for cytokinesis in fission yeast, is a component of the cell division ring and interacts with profilin. J. Cell Biol. *137*, 169–182.
32. Shaner, N.C., Campbell, R.E., Steinbach, P.A., Giepmans, B.N., Palmer, A.E., and Tsien, R.Y. (2004). Improved monomeric red, orange and yellow fluorescent proteins derived from Discosoma sp. red fluorescent protein. Nat. Biotechnol. *22*, 1567–1572.
33. Glynn, J.M., Lustig, R.J., Berlin, A., and Chang, F. (2001). Role of bud6p and tea1p in the interaction between actin and microtubules for the establishment of cell polarity in fission yeast. Curr. Biol. *11*, 836–845.
34. Harris, E.S., Rouiller, I., Hanein, D., and Higgs, H.N. (2006). Mechanistic differences in actin bundling activity of two mammalian formins, FRL1 and mDia2. J. Biol. Chem. *281*, 14383–14392.
35. Moseley, J.B., and Goode, B.L. (2005). Differential activities and regulation of Saccharomyces cerevisiae formin proteins Bni1 and Bnr1 by Bud6. J. Biol. Chem. *280*, 28023–28033.
36. Pollard, T.D., Blanchoin, L., and Mullins, R.D. (2000). Molecular mechanisms controlling actin filament dynamics in nonmuscle cells. Annu. Rev. Biophys. Biomol. Struct. *29*, 545–576.
37. Sirotkin, V., Beltzner, C.C., Marchand, J.B., and Pollard, T.D. (2005). Interactions of WASp, myosin-I, and verprolin with Arp2/3 complex during actin patch assembly in fission yeast. J. Cell Biol. *170*, 637–648.
38. Fehrenbacher, K.L., Yang, H.C., Gay, A.C., Huckaba, T.M., and Pon, L.A. (2004). Live cell imaging of mitochondrial movement along actin cables in budding yeast. Curr. Biol. *14*, 1996–2004.
39. Wu, J.Q., and Pollard, T.D. (2005). Counting cytokinesis proteins globally and locally in fission yeast. Science *310*, 310–314.